Science Advances

Supplementary Materials for

The crystal structure of the global anaerobic transcriptional regulator FNR explains its extremely fine-tuned monomer-dimer equilibrium

Anne Volbeda, Claudine Darnault, Oriane Renoux, Yvain Nicolet, Juan C. Fontecilla-Camps

The PDF file includes:

Materials and Methods
Fig. S1. Stereo view of the electron density of the N-terminal region of holo-FNR (starting at His[19]), shown as a black mesh contoured at 1σ.
Fig. S2. Comparison of the α-C helical dimerization interfaces of FNR and other selected CRP-family members, using deposited structures at the Protein Data Bank.
Fig. S3. Stereo image viewed down the dimer twofold axis.
Fig. S4. Stereo image of the electron density near the center of the dimer interface.
Fig. S5. Stereo image of the superposition of FNR (purple) to FixK$_2$ (green) showing the similar position and orientation of the DNA binding α-F helices at the bottom of the figure.
Table S1. X-ray data and refinement statistics.
References (*24–33*)

Materials and Methods

Expression vector for *Af*FNR. The synthetic gene of *Af*FNR (GenBank ID ACH67249.1) was purchased from Genscript™. The DNA sequence was codon optimized for expression in *Escherichia coli* and inserted into a pET-15b expression vector (Novagen™) between the NcoI and BamHI restriction sites. A streptavidin-tag was subsequently inserted between methionine 1 and serine 2 by PCR following the QuikChange® strategy, using the following primers: *forward* 5´-CACCCGCAGTTCGAAAAGGCAAGCAGTGATAACAGCGCAAATAAACG-3´ and *reverse* 5´-CTTTTCGAACTGCGGGTGGCTCCACATGGTATATCTCCTTCTTAAAGTTAAACAAAA-3´ and Phusion™ polymerase. The integrity of the construction was verified by sequencing the entire gene. This led to a pStrep*Af*FNR construct with the following sequence:

ATGTGGAGCCACCCGCAGTTCGAAAAGGCAAGCAGTGATAACAGCGCAAATAAACGTATCCAGA
GCGGCGGTTGCGCCATTCATTGCCAGGATTGTAGCATTTCTCAGCTGTGTATCCCGTTCACCCT
GAACGATTCTGAACTGGATCAGCTGGATGAAATTATCGAACGTAAAAAACCGATCCAGAAAGGC
CAGGAACTGTTTAAAGCGGGTGATGAACTGAAATGCCTGTATGCCATTCGCTCTGGCACCATCA
AAAGTTACACCATTACGGAACAGGGTGATGAACAGATCACGGCATTCCATCTGGCGGGCGATCT
GGTGGGTTTTGATGCCATTACCGAAGCACAGCACCCGAGCTTTGCACAGGCGCTGGAAACGTCT
ATGGTTTGTGAAATTCCGTATGAAATCCTGGATGATCTGAGCGGCAAAATGCCGAAACTGCGTC
AGCAGATTATGCGCCTGATGTCTAATGAAATCAAAGGTGATCAGGAAATGATTCTGCTGCTGAG
CAAGAAAAACGCGGAAGAACGTCTGGCGGCCTTCCTGTACAATCTGAGTACCCGTTTTCATCAG
CGCGGCTTCAGCCCGCGTGAATTTCGCCTGACCATGACGCGCGGCGATATCGGTAACTATCTGG
GCCTGACCGTGGAAACGATTAGCCGTCTGCTGGGTCGCTTTCAGAAAACCGAAATGCTGACGGT
TAAAGGCAAATACATTACCATCAATGATCACGATGCCCTGGCAGAACTGGCGGGTAGCGCCAAA
GAAATTAAATAATGA, which corresponds to the following protein sequence:

MWSHPQFEKASSDNSANKRIQSGGCAIHCQDCSISQLCIPFTLNDSELDQLDEIIERKKPIQKG
QELFKAGDELKCLYAIRSGTIKSYTITEQGDEQITAFHLAGDLVGFDAITEAQHPSFAQALETS
MVCEIPYEILDDLSGKMPKLRQQIMRLMSNEIKGDQEMILLLSKKNAEERLAAFLYNLSTRFHQ
RGFSPREFRLTMTRGDIGNYLGLTVETISRLLGRFQKTEMLTVKGKYITINDHDALAELAGSAK
EIK.

Anaerobic culture of AfFNR using BL21 *Escherichia coli* cells transformed with the pRSF-ISC-MetK plasmid (*24*). Cells were grown in a glove box at 20°C with addition of fumarate, cysteine, methionine and iron citrate. The induction was carried out by addition of IPTG

(isopropyl β-D-1-thiogalactopyranoside) when the cultures reached an $OD_{600} = 1$. After overnight growth in the glove box, cells were pelleted by centrifugation for 15 min at 6000 rpm and then stored at -80 °C.

Protein purification. The pelleted cells were thawed, resuspended in tampon A (50 mM Tris pH 8, 300 mM NaCl) and disrupted by sonication in the glove box. Next, the sonicated sample was centrifuged for 45 min at 15,000 rpm and the supernatant was injected to a Strep-tactin superflow column (10 ml, IBA®) (Akta purifier, GE) previously equilibrated with 100 mM Tris pH 10, 150 mM NaCl. The column was then washed with 6 column volumes of tampon A in the glove box followed by 3 column volumes of tampon A + 2.5 mM desthiobiotine. Fractions containing purified *Af*FNR, as verified by SDS-PAGE, were pooled and shown to contain a total of 16.3 mg of protein in 51 mL (determined by the Rose Bengal method (*25*). After about 8-fold concentration by ultrafiltration the protein solution was applied to a Superdex 200 Hiload 16/60 (120mL) column previously equilibrated with tampon A + 2 mM DTT. After verification of the protein purity by SDS-PAGE, a volume of 47 mL was obtained by pooling the relevant fractions. The total amount of protein was 15.51 mg as determined by the Rose Bengal method. *Af*FNR was then concentrated by ultrafiltration with tampon A to 2.5 mg/ml and frozen in liquid N_2 in either 100 μL or 500 μL aliquots.

Preparation of an *Af*FNR sample for aerobic studies. A 500 μL aliquot of *Af*FNR prepared as described in the *Protein purification* paragraph was thawed and diluted to 0.5 mg/mL with tampon A + 2 mM β-mercaptoethanol in the glove box (the latter was used to prevent protein aggregation). 180 μL of this solution were then poured into a cuvette that was then sealed and taken out of the glove box.

Stability of the [4Fe-4S] cluster as a function of time upon air exposure. UV/visible spectra of the previous sample were recorded after being exposed to air at t = 0, 15 min, 60 min, 330 min, and overnight. Selected times are shown in Fig. 1A.

Dimer-monomer equilibrium as a function of time upon air exposure. The stability of the starting dimeric anaerobic *Af*FNR was determined by size-exclusion chromatography using a calibrated Superdex 200 HR 10/30 column (GE) using a sample prepared as described above. The protein was eluted using tampon A + 2 mM β-mercaptoethanol. After overnight exposure to air *Af*FNR was mostly monomeric. Conversely, an identical anaerobic sample applied to a

Superdex 200 HR 10/30 column inside the glove box was dimeric. These results are summarized in Fig. 1B.

Crystallization. Initial *Af*FNR crystals were obtained using the sitting drop vapor diffusion method and a high throughput screening strategy with a Gryphon robot (*AriRobbins*, CA, USA) inside a glove box. Thin brown plates were thereafter manually obtained from 1:1 mixtures of a solution containing 50 mM Tris base, pH 8.0, 30 mM NaCl, 2 mM dithionite and 5 mg/mL of anaerobically prepared *Af*FNR and crystallization solutions composed of 16 to 18% methyl pentanediol, 100 mM MES, pH 6 to 6.6 and 25 mM LiCl. Because some crystals contained degraded iron-sulfur clusters (see text and Table S1) 2 mM dithionite were added to subsequent assays.

X-ray data collection and structure determination. All the X-ray data used here were collected at the European Synchrotron Radiation Facility (ESRF) in Grenoble, at beam lines BM30A, ID23eh1 and ID23eh2. Initially, two data sets were collected at BM30A at $\lambda = 0.97972$ and $\lambda = 1.74147$Å to 3.15 Å and 3.3 Å resolution, respectively. Fe absorption edge spectra of FNR crystals were measured with a Roentec X-Flash multi channel analyzer. The program *CHOOCH* (*26*) was then used to select the X-ray wavelength providing the maximal iron anomalous signal for the 3.15 Å resolution data. X-ray diffraction data were indexed, integrated and scaled with *XDS* (*27*). A final scaling and merging step was performed with the *AIMLESS* program (*28*) of the *CCP4* package (*29*). X-ray data statistics for the crystals used are given in Table S1. A molecular replacement (MR) solution for FNR was obtained with the program PHASER (*30*), using the related FixK$_2$ structure (*17*), which has 24% amino acid sequence identity to *Af*FNR, as a search model. This solution was confirmed by the presence of a significant peak in a 5 Å resolution MR-phased anomalous electron density difference map close to the Cys122 thiolate, a known ligand of the [4Fe-4S] cluster (*1*). Initial structure refinement was performed with *REFMAC5* (*31*), using *COOT* (*32*) for manual model corrections. In order to improve the resolution, we then rapidly collected highly redundant holo-FNR X-ray data from three volumes of the same tetragonal I422 crystal taking advantage of the high beam intensity at the ID23eh2 microfocus beam line. This procedure allowed us to collect 120° of data for each volume within 80 sec on a Pilatus detector, and extended the resolution to 2.65 Å. Due to the intrinsic disorder of our crystals the data were very weak in the highest resolution shell. However, the corresponding CC$_{1/2}$ correlation coefficient between random half data sets was still

significant (Table S1), which justified the choice of resolution cutoff (*28*). In addition, we collected data from the same crystal at the Fe absorption edge and used the hybrid substructure search in the *PHENIX* package (*33*) to obtain independent single anomalous dispersion (SAD) phase information. After combining molecular replacement and SAD phases using the MR-SAD Phaser mode in *PHENIX* an interpretable electron density map could be obtained for most of the more disordered parts of the N-terminal region of holo-FNR. We also used *PHENIX* for the final refinement of atomic positions (xyz) and grouped B-factors, including refinement of TLS groups that were automatically selected by the program (*33*). Final refinement statistics are given in table S1.
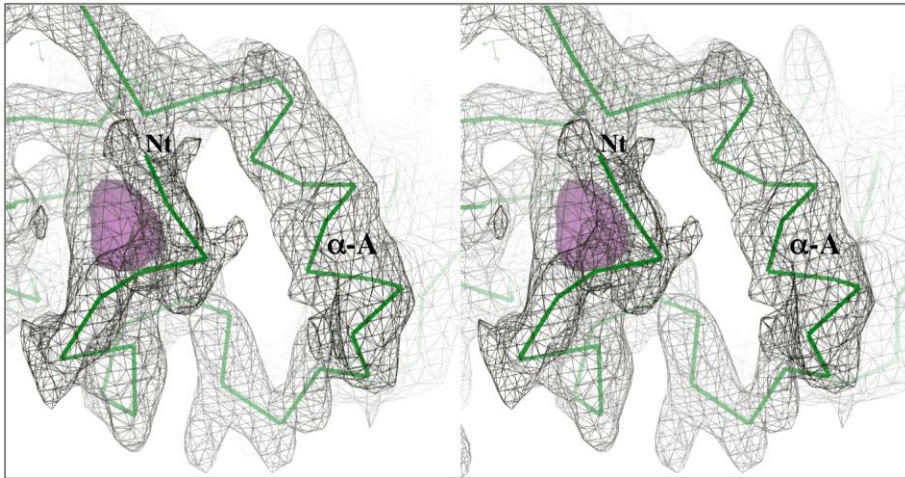
Figures

Fig. S1. Stereo view of the electron density of the N-terminal region of holo-FNR (starting at His[19]), shown as a black mesh contoured at 1σ. The corresponding anomalous difference map is shown as a pink peak contoured at 7σ as in Fig 1C. The Cα-trace of the main chain is depicted in green.
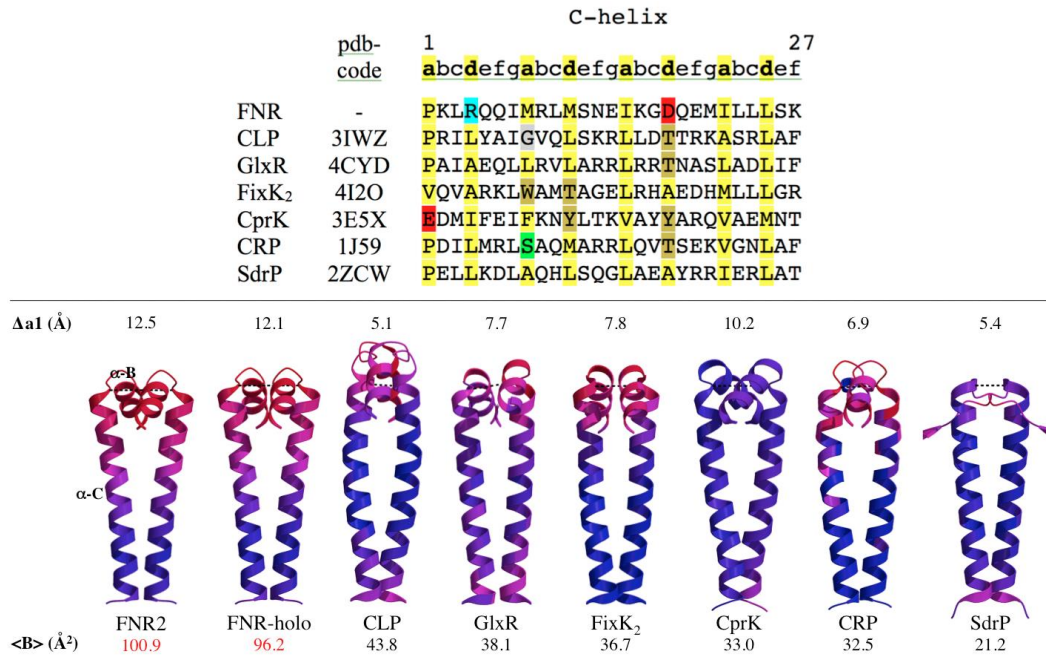
Fig. S2. Comparison of the α-C helical dimerization interfaces of FNR and other selected CRP-family members, using deposited structures at the Protein Data Bank. In the sequence comparison the positions labeled **a** and **d** face the **d'** and **a'** positions of the same helix in the opposite monomer (see Fig. 4D). A unique feature of FNR is the presence of charged residues at **d**4 and **d**18. In the structures shown below the α-B helix (if present) is also included. These structures are colored according to increasing temperature (B-) factor values, from 0.5<B> (blue) to 1.5<B> (red), with <B> (average B-value for the complete structure) given below the figures. Separations between **a**1 and **a**1' positions (Δa1) are also indicated. This analysis shows that FNR is the only member of the family that combines a large Δa1 with a high degree of disorder, underscoring the inherent instability of the FNR-dimer.
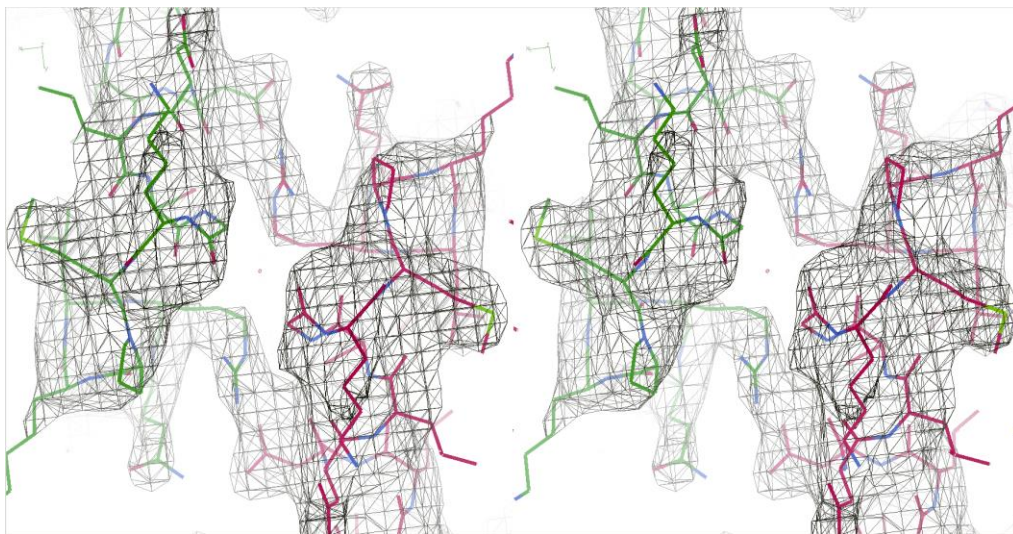
Fig. S3. Stereo image viewed down the dimer twofold axis. Note the electron density connecting the two Asp130-Arg140 salt bridges at the background. This figure corresponds to Fig. 4B of the main text.
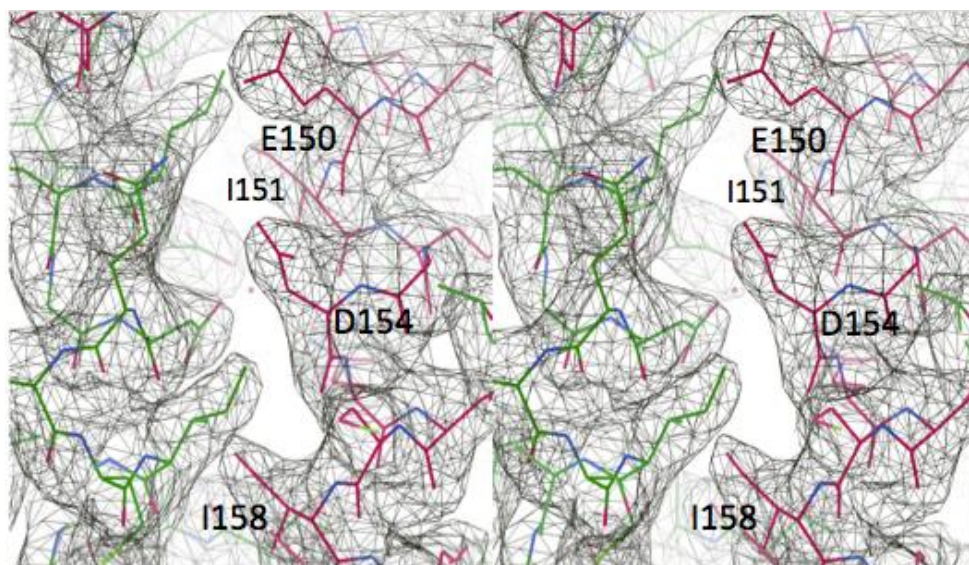

Fig. S4. Stereo image of the electron density near the center of the dimer interface. Residues discussed in the main text are labeled. This figure corresponds to Fig. 4C of the main text.
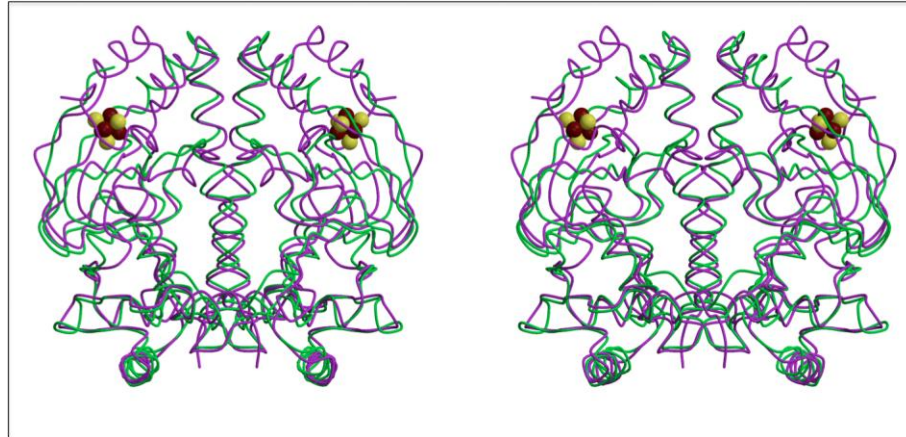
Fig. S5. Stereo image of the superposition of FNR (purple) to FixK$_2$ (green) showing the similar position and orientation of the DNA binding α-F helices at the bottom of the figure.

Table S1. X-ray data and refinement statistics.

Crystal	Holo-FNR	Holo-FNR	FNR2[#]
Data collection			
ESRF beamline	ID23eh2	BM30a	ID23eh1
Wavelength (Å)	*0.87260*	*1.74028*	*0.97242*
Space group	*I422*	*I422*	*I422*
Cell dimensions: a, b, c (Å)	75.2, 75.2, 218.1	75.5, 75.5, 218.1	75.3, 75.3, 212.4
Molecules/asymmetric unit	1	1	1
Resolution (Å)	47.9-2.65 (2.74-2.65)	47.9-2.65 (2.75-2.65)	47.6-2.60 (2.69-2.60)
Measured reflections	244263 (23228)	97063 (9176)	126067 (12722)
Unique reflections	9609 (899)	9524 (900)	9847 (938)
Redundancy	25.4 (25.8)	10.2 (10.2)	12.8 (13.6)
Completeness (%)	99.8 (97.9)	98.4 (98.1)	99.9 (99.9)
R_{merge} (%)*	17.2 (438.9)	10.1 (371.8)	9.1 (240.7)
R_{pim} (%)*	4.8 (123.3)	4.5 (170.5)	3.7 (95.3)
$CC_{1/2}$*	0.997 (0.376)	0.997 (0.340)	1.000 (0.586)
$<I/\sigma_I>$	14.2 (1.0)	18.3 (0.7)	21.1 (1.3)
Refinement			
Resolution (Å)	47.9-2.65		37.6-2.6
Number of reflections	17484		17948
R_{work} (%)	18.8		19.1
R_{free} (%)	24.2		23.7
Number of atoms			
All	1795		1626
Fe (in FeS cluster)	4		2
S (in FeS cluster)	4		2
Water	0		8
Others (in MPD)	16		24
Number of TLS groups	4		10
Average B-factors ($Å^2$)			
Domain 1 (Nt-126)	108.3		114.6
Domain 2 (127-163)	101.1		108.1
Domain 3 (164-248)	79.9		85.1
R.m.s. deviations			
Bond lengths (Å)	0.013		0.009
Bond angles (°)	1.5		1.2
Ramachandran plot statistics (%)			
Most favored	89.0		92.6
Allowed	11.0		6.9
Disallowed	0.0		0.5

* as defined in (*28*);

Although the crystals used to solve the two structures were grown and flash-cooled under equivalent anaerobic conditions, the one with degraded cluster (FNR2) sat in the glove box over two months prior to flash cooling.

Conversely, the crystal containing holo-*Af*FNR was flash-cooled only 8 days after setting the crystallization drops. We have already observed long-term iron-cluster degradation at about 1ppm O_2 (*22*) and here we speculate that slow O_2 release from plastic ware within the glove box may be responsible for this effect.

$ Bijvoet pairs were treated as independent observations. This allowed the inclusion of the anomalous contributions from Fe and S atoms in the refinement procedure, which gave significantly improved refinement statistics.